Nanoscale

Dynamic Article Links

Cite this: *Nanoscale*, 2011, **3**, 3805

www.rsc.org/nanoscale

PAPER

The critical role of water in spider silk and its consequence for protein mechanics

Cameron P. Brown,[*abcd] Jennifer MacLeod,[b] Heinz Amenitsch,[e] Fernando Cacho-Nerin,[e] Harinderjit S. Gill,[a] Andrew J. Price,[a] Enrico Traversa,[cf] Silvia Licoccia[cd] and Federico Rosei[cd]

Received 17th May 2011, Accepted 29th June 2011
DOI: 10.1039/c1nr10502g

Due to its remarkable mechanical and biological properties, there is considerable interest in understanding, and replicating, spider silk's stress-processing mechanisms and structure-function relationships. Here, we investigate the role of water in the nanoscale mechanics of the different regions in the spider silk fibre, and their relative contributions to stress processing. We propose that the inner core region, rich in spidroin II, retains water due to its inherent disorder, thereby providing a mechanism to dissipate energy as it breaks a sacrificial amide-water bond and gains order under strain, forming a stronger amide-amide bond. The spidroin I-rich outer core is more ordered under ambient conditions and is inherently stiffer and stronger, yet does not on its own provide high toughness. The markedly different interactions of the two proteins with water, and their distribution across the fibre, produce a stiffness differential and provide a balance between stiffness, strength and toughness under ambient conditions. Under wet conditions, this balance is destroyed as the stiff outer core material reverts to the behaviour of the inner core.

Introduction

The mechanical properties of spider silk originate from the core of the fibre, which is protected by a series of 'skin' layers[1] (Fig. 1). The outer core (≈15% of the radius) is thought to consist mainly of the highly ordered protein Spidroin I, with the inner core (≈80% of the radius) consisting of both Spidroin I and the less-ordered Spidroin II.[1,2] The hierarchical structure of spider silk is shown in Fig. 2. The intrinsic disorder in Spidroin II occurs due to the presence of proline, which twists away from simple, ordered configurations.[3] This combination of proteins results in a distribution of approximately 40% ordered domains (two hydrogen bonds per amide group), 15% permanently disordered domains (one hydrogen bond per amide group) and 45% intrinsically disordered domains but with potential for order.[3,4] Although the degree of order has a considerable influence on the strength, stiffness and elasticity,[5] the interactions between the ordered and disordered domains are also critical.[6,7]

An important factor in the ordering, and therefore mechanics, of spider silk fibres is water. In addition to understanding the structure-function properties of the material, the change in structure and mechanics upon wetting is particularly important for biomedical applications of spider silk, which involves an inherently wet environment. A number of studies of the bulk response of spider silk to water have, therefore, been undertaken using techniques such as tensile testing,[8] often in combination with other techniques such as X-ray scattering,[9] vibrational spectroscopy,[10] neutron scattering[11] and nuclear magnetic resonance (NMR).[12] These bulk fibre studies have shown that water

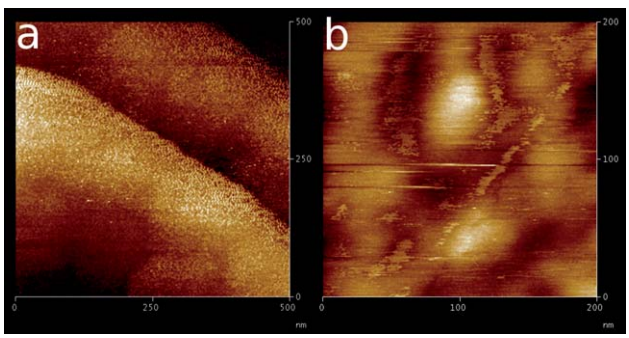

Fig. 1 AFM height image of spider silk fibre cross-section. (a) two skin layers, with the centre of the fibre towards the bottom-left of the image; (b) core region showing globular morphology.

[a]*Botnar Research Centre, University of Oxford, Oxford, UK. E-mail: cameron.brown@ndorms.ox.ac.uk*
[b]*Centro NAST, Dipartimento di Scienze e Tecnologie Chimiche, Università di Roma Tor Vergata, via Della Ricerca Scientifica, 000133 Roma, Italy*
[c]*Institut National de la Recherche Scientifique, Université du Québec, 1650 boulevard Lionel-Boulet, Varennes, QC, Canada. E-mail: rosei@emt.inrs.ca*
[d]*Italy-Quebec Joint Laboratory in Nanostructured Materials for Energy, Catalysis and Biomedical Applications.*
[e]*Institute for Biophysics and Nanosystems Research, Schmiedlstr. 6, 8042 Graz, Austria*
[f]*International Research Center for Materials Nanoarchitectonics, National Institute for Materials Science, 1-1 Namiki, Tsukuba, Ibaraki, 305-0044, Japan*

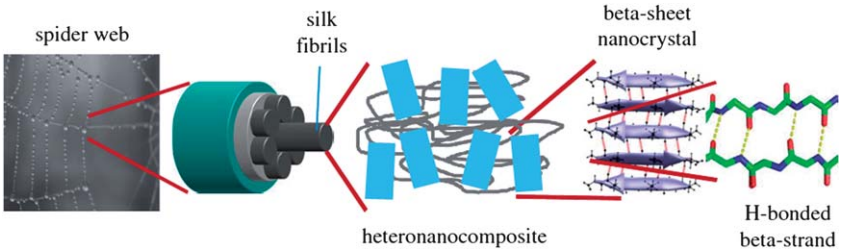

Fig. 2 Hierarchical structure of spider silk. Reproduced with permission from ref. 40.

infiltrates disordered domains, decreasing the alignment of the ordered domains and contracting the fibre, yet our understanding of the response of different components, and the distribution of this response across the spider silk fibre, is lacking.

The distribution of Spidroin I and II in the different layers of spider silk provide a means by which their separate roles and interactions can be studied on a level of hierarchy above that of single-protein unfolding[13] and below that of bulk mechanical analysis.[14] Here, we probe the nanoscale mechanical properties of the core material *in situ*, using atomic force microscopy (AFM) to mechanically investigate the roles of the two proteins and the influence of water on their respective behaviours. X-ray scattering was then used to determine the relative influence of water on the ordered and disordered domains. We find that water plays a dominant role in the mechanics of fibre, even under ambient conditions.

Methods

Major ampulate spider silk was harvested from a single Nephila clavipes (golden orb weaver) web in Redland Bay, Australia, the morning after spinning. The fibres were spun at approximately 60% relative humidity (RH) and collected at approximately 70% RH. The fibres were fixed at their ends with adhesive tape, maintaining their length at the time of collection. Nephila clavipes was chosen for ease of handling due to its red-gold colour and for consistency with the literature, which predominantly uses the genus Nephila. A bundle of approximately 30 fibres was mounted in paraffin, cut into 5 μm cross-sections by microtome (RM2155, Leica Mikrosysteme GmbH, Austria) and mounted on a platinum plated silicon wafer. The paraffin was then removed by a sequence of 3 dips in citrisolve followed by a citrisolve/ethanol mixture and a gradual rehydration in a series of distilled water/ethanol mixtures. The samples were left to equilibrate overnight at approximately 60% RH and 24 °C, leaving an array of samples. The ability to remove paraffin from the samples after sectioning provides a significant advantage over other standard cutting media such as epon and LR-white,[1] which penetrate the material and harden, thus altering its mechanical properties.

Six sections were imaged in tapping mode (see Fig. 3) before being subjected to indentation with an atomic force microscope under ambient conditions (Enviroscope, Veeco Instruments Inc., USA), first in its equilibrated state at 60% RH, then immediately after 10 min immersion in distilled water, and again after reaching equilibrium overnight. Indentation was performed to a depth of approximately 50 nm, with a tip of nominal radius 15 nm (VISTAprobes T300; ≈10 nm radius before testing and 20 nm after). The cantilever had a resonant frequency of 298 kHz, from which the spring constant was calculated to be 40 N m^{-1}, by interpolating empirical values supplied by the manufacturer. A possible limitation of this technique is that by cutting the fibres, any pretension in the axial direction will be lost, potentially affecting the mechanical behaviour at the cut surface.

A second group of approximately 100 fibres was cut into a 15 mm length and fixed to a cardboard frame relaxed under 20% RH, forming a bundle of approximately 200 μm diameter. Small and wide angle X-ray scattering patterns were taken with the sample mounted (meridonal direction horizontally) in a closed environmental box at <1, 20, 40, 60, 80 and >99% RH measured with a humidity sensor (Hydroclip IE-1, Rotronic AG, Bassersdorf, Switzerland), at the SAXS beamline of the ELETTRA synchrotron radiation facility, Trieste, Italy.[15] Humidity was controlled using a mixture of dry and wet air. The sample was hydrated in steps, with each step held for 20 min before measurements were taken. This was repeated three times down the length of the fibre bundle.

The X-ray scattering patterns were collected from a spot size of 200 × 50 μm^2 at each position. A Mar300 Image Plate detector with a circular active area of 300 mm in diameter was used to acquire the patterns, which were processed using FIT2D Software[16] and IGOR Pro (WaveMetrics, Oregon, USA). One-dimensional (1-D) profiles were obtained using an azimuthal integration over the region containing the reflections. The data were corrected for dark counts and background, and normalized to the region 6 $nm^{-1} < Q < 7$ nm^{-1}.

The a and b dimensions were determined from analysis of the [200] and [120] reflections, respectively. For an orthorhombic structure, the unit cell dimensions a, b and c relate to the lattice spacing d for a particular set of Miller indices (hkl) as:

$$\frac{1}{d_{hkl}^2} = \frac{h^2}{a^2} + \frac{k^2}{b^2} + \frac{l^2}{c^2}$$

a can be extracted directly from the position of the 200 reflection, as $a = 2d_{200}$. Determination of b relies on both the value of a determined from (200) and the position of the (200) peak, since:

$$\frac{1}{d_{120}^2} = \frac{1^2}{a^2} + \frac{2^2}{b^2}$$

The FWHM of the [200] and [120] reflections, ΔQ_{hkl}, can be used to determine the corresponding crystallite sizes, L_{hkl} according to the Debye-Scherrer equation:

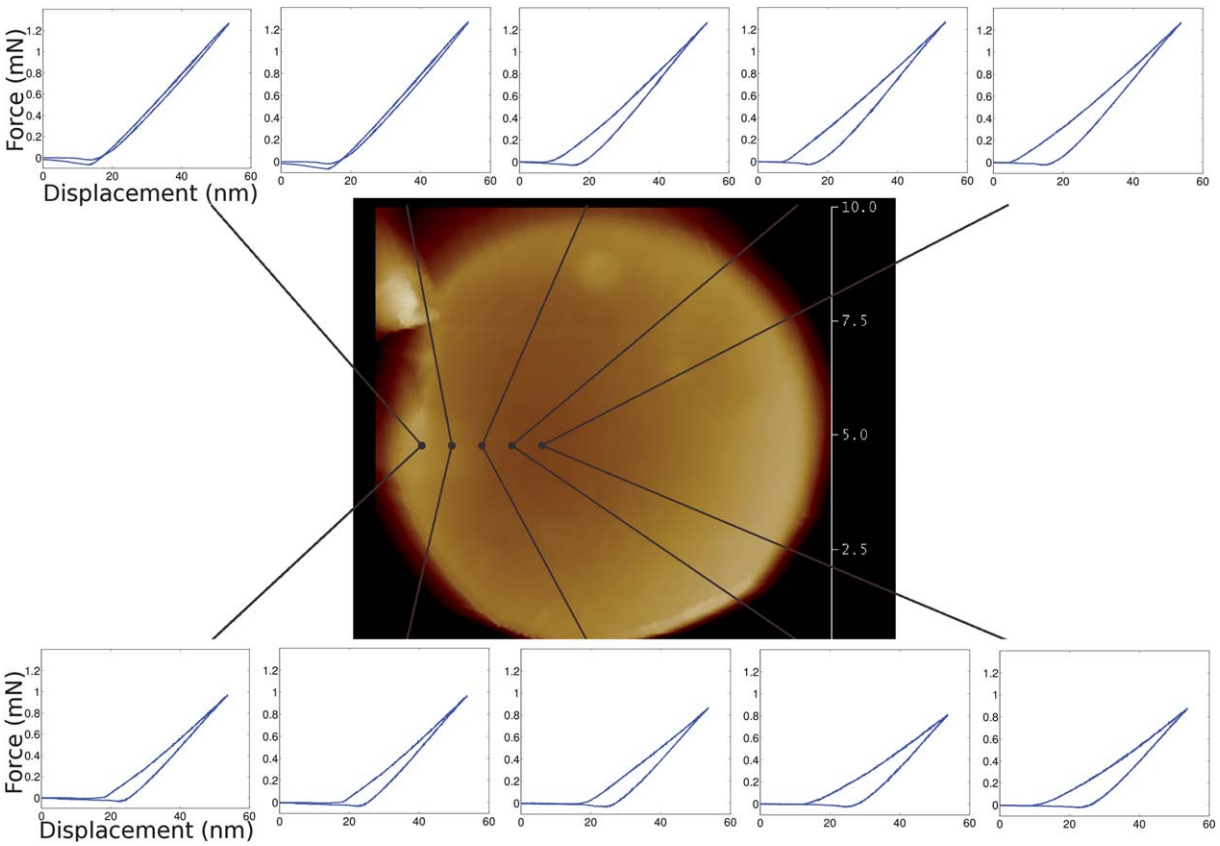

Fig. 3 AFM image of cross-sectioned fibre with the profile of force-displacement curves from the outer to inner regions shown under ambient (top) and wet (bottom) conditions. The scale bar on the right of the AFM image is in microns, and the axes of the force-displacement graphs are constant with *y*-axes from 0 to 1.2 mN and *x*-axes from 0 to 60 nm.

$$L_{hkl} = \frac{k4\pi}{\Delta Q_{hkl}}$$

in which k is a scaling constant taking into account the form-factor of the crystallites.

Results

Under ambient conditions, the mechanical behaviour varied with position on the cross-section (Fig. 3, top). The highly ordered outer core exhibited a purely elastic behaviour, with the unloading curve closely following the loading curve. The inner core showed a distinct 'plastic' effect, whereby some of the applied energy was dissipated and the strain not recovered. Although the outer-core silk showed considerably more resistance to indentation than silk from the inner core (22%, given by the slope of the force-displacement curves in Fig. 4), the first few nanometres of unloading, to which elastic properties are usually attributed,[17] were very similar (within 5%) in the two regions.

After immersion in water (Fig. 3, bottom), the behaviour of the inner core changed little: a lower indentation stiffness (23 ± 10%) and a slightly decreased elastic recovery (7 ± 3%) during unloading, compared to ambient conditions. The outer core, however, showed a radically different load-unload profile, changing from a purely elastic response to a highly plastic behaviour, similar to that of the inner core under ambient conditions. It is also interesting to note that the slopes of the unloading curves were remarkably similar (within 3%) for the wet inner and outer and core material (Fig. 4b).

The small (SAXS) and wide (WAXS) angle X-ray scattering experiments (Fig. 4a, 4b, 5) showed no change in crystal size with increasing hydration. Based on the conventions set forth by Warwicker,[18] the orthorhombic unit cell of the crystallites is designated to have its c-axis along the direction of the fibre, with its a- and b-axes distributed randomly around the fibre axis.[19] As we measured only the [120] and [200] reflections, only the dimensions along the side chains (a-axis) and along the hydrogen-bonds between the pleated sheets (b-axis) were investigated. It is in these directions, however, that swelling is expected to occur.

Fig. 5 shows the average of the three data sets collected in the SAXS/WAXS experiments. The data were collected along the equatorial direction, and exhibit the expected peaks corresponding to the [120] and [200] reflections (inset). The positions and shapes of the peaks are not significantly sensitive to humidity; however, humidity dependent changes can be observed in both the low-Q (SAXS) region and the very high-Q region, as well as in the intensity of the peaks. In the case of the SAXS data, the curves exhibit broadening and increased intensity above 80% humidity, which indicates an increased contrast between the amorphous and crystalline zones consistent with water uptake in the amorphous component.[20] In the case of the high-Q

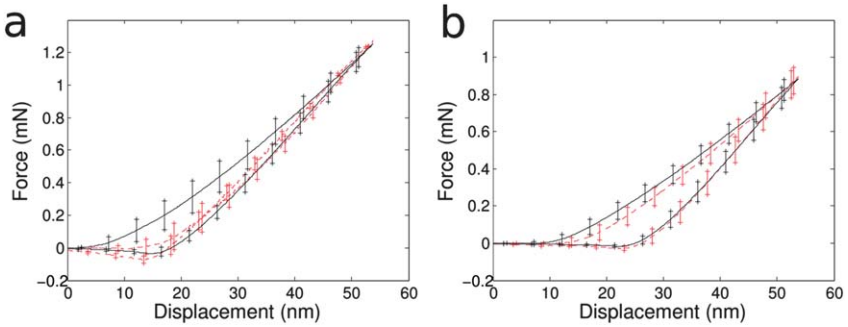

Fig. 4 Average indentation force-displacement curves under ambient (a) and dry (b) conditions. Black lines represent inner core material; red, dashed lines represent outer core material.

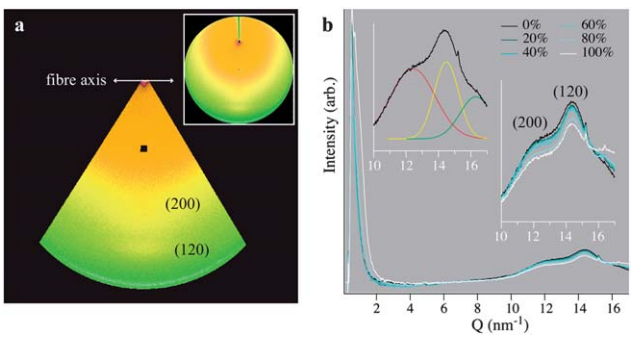

Fig. 5 (a) Masked scattering data, indicating the integrated region used to obtain SAXS/WAXS profiles. The (200) and (120) peaks are indicated, along with the fibre axis direction and location. The inset shows the entire scattering pattern. (b) Integrated average SAXS/WAXS profiles for RH varying from 0–100%. The inset at right shows an enlarged view of the WAXS region, with the (200) and (120) peaks indicated. The inset at left shows a typical set of Gaussian fits, comprising the (200) peak (red), the (120) peak (yellow) and the amorphous water peak (green).

data ($Q > 16$ nm^{-1}), the intensity increases systematically with humidity. As in previous studies,[20,21] we attribute the intensity at high Q values to scattering from disordered water, and accordingly fit this contribution with an additional Gaussian peak profile. The [200] and [120] reflections were fit simultaneously using Gaussian peak profiles. When freely fit simultaneously with the [200] and [120] reflection, this peak is consistently located at $Q = 16.3$ nm^{-1}.

Plots of the humidity-dependent data are presented in Fig. 6. The unit cell parameters (Fig. 6a) are insensitive to humidity and in agreement with previous studies on supercontracted spider silk.[20,22] The average cell parameters determined from the [200] and [120] reflections are $a = 1.008 \pm 0.008$ nm and $b = 0.966 \pm 0.001$ nm, respectively. The Debye-Scherrer crystallite sizes along both [120] and [200] are similarly insensitive to humidity (Fig. 6b), though a small, statistically insignificant swelling trend was observed in the direction along the hydrogen-bonds between the pleated β-sheets. It is also interesting to note the increase in unit cell parameter *a* from dry to 20% RH. We found minimum average crystallite sizes of 3.1 and 7.3 nm along these respective directions, consistent with previous reports of anisotropic crystallites.[20] This size is smaller than the radius of the AFM tip and the displacements applied during indentation.

Discussion

This study aimed to investigate the mechanical effect of water on different regions of the spider silk fibre, and therefore on the two major proteins, using AFM indentation and X-ray scattering. We found that the inner core region, rich in spidroin II, retains water due to its inherent disorder, arguing that this dissipates energy through the breaking of a sacrificial amide-water bond and increasing its order under strain. The outer core, rich in spidroin I, is more ordered under ambient conditions and is inherently stiffer and stronger, yet does not on its own provide high toughness. When the distribution of these effects is considered across the fibre, we propose that the tough inner core and stiff outer core combine to produce a highly resilient material under ambient conditions. In wet conditions, however, the outer core behaviour changes to that of the inner core, weakening the fibre as a whole.

We interpret the 'plastic' effect in Fig. 2 and 3 as resulting from the level of disorder, which is known to be both intrinsic to the Spidroin II in the inner core due to the presence of proline,[3] and forced by immersion of the fibre in water[23] (see the change in ordered fraction and crystallite swelling in Fig. 4 and 5). The induced strain from the indentation, when transferred to the protein level, will push/pull some of the disordered domains into an ordered configuration, preventing the material from recovering elastically. The amount of reconfiguration is difficult to quantify due to the complex nanoscale structure of spider silk, but for a given structural arrangement and constant indentation conditions, is proportional to the area between the loading and unloading curves, and therefore proportional to the amount of energy dissipated during the indentation. This energy is roughly equal to the product of the energy per hydrogen bond and the number of hydrogen bonds broken, with the weaker bonds breaking first. With the correct (tight) packing conditions, a similar effect is likely to be observed under tension.[3]

During spinning, most of the water is expelled from the aqueous protein solution (70% water);[24,25] the highly hydrophobic, ordered domains expel all of their water but, as inferred from IR spectra,[26] some water remains in the less hydrophobic, disordered domains. The higher shear stresses in the outer fibre during extrusion will arguably lead to the formation of more ordered domains compared to the inner regions, similar to the increased order and orientation resulting from the higher stresses during fast extrusion.[27] Concurrently, water would be forced out

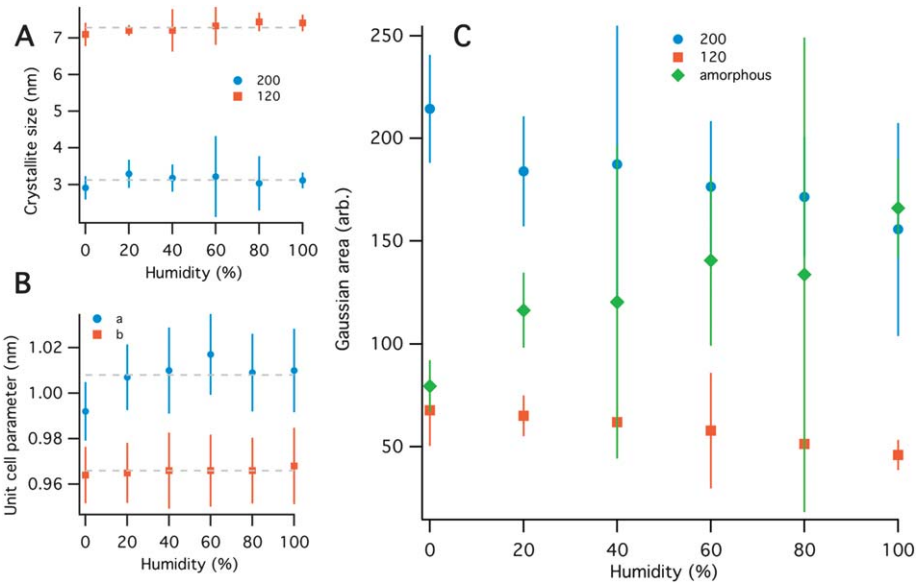

Fig. 6 Fits of the data in Fig. 4. Crystallite size calculated from the Debye-Scherrer equation (a), unit cell parameters (b), and integrated intensity of the peaks (c).

of the structure in these highly stressed outer regions, but less so from the inner regions. The disorder due to water results from it acquiring hydrogen bonds between the molecular chains in the fibre's oriented amorphous domains,[23] which are easier to penetrate than the hydrophobic, crystalline domains such as β-sheets.[28]

The integrated intensity of the [120] and [200] peaks (Fig. 5c) is related to the degree of crystallinity of the fibre. Water is known to significantly reduce the volume fraction of the crystalline component in spider silk due to uptake in the amorphous domains,[29] yet bulk cyclic loading experiments and modelling suggest that the ordered phase of a specific fraction of the peptide segments can be manipulated by exposure to water.[3] The decrease in the integrated intensities of the [120] and [200] reflections, and the increase in the intensity of the amorphous peak (Fig. 4b, 5c), confirm a decrease in the volume fraction of ordered domains with humidity.

Through the same mechanism as for intrinsic disorder described above, the disordering of the structure caused by the infiltration of water (Fig. 6c) would be reversed, and forced back into an ordered configuration under an applied load. This raises some interesting questions; particularly whether the water in the disordered domains plays an equal or even superior part to that of the proline[30] and if so, whether the main mechanical function of the proline is to enable the action of water.

We propose that under ambient conditions, the bound water between protein chains in the inner core will be pushed out under an applied load, allowing reconfiguration due to sacrificial bonding. Once the load is withdrawn, however, the now unbound water can reacquire some of the hydrogen bonds, allowing a partial recovery. This is essentially a self-repair mechanism, much like the repair of hydrogen bonded rubber,[31] but is controlled by water. As more bonds are taken up by water, a greater reconfiguration is possible, resulting in softening and a decreased elastic recovery (Fig. 4). The observed softening, we propose, is due to the amide-water bonds being weaker than the amide-amide bonds that they replace.[24] The decreased recovery will result from the combination of decreased order and the lower stress required for reconfiguration. Water-controlled recovery will be slower than the entropy-driven elastic recovery as it will take time for the water to infiltrate the more-ordered structures. The effect of this slow recovery can be seen when scanning 30 min after indentation, at which time the residual indentations are no longer observed. The timescale of water-driven recovery is in good agreement with stress relaxation data from bulk fibres,[14] which show >95% relaxation after 30 min, and full relaxation at approximately 80 min.

The role of water in the intrinsically disordered inner core structure leads us to consider the behaviour of the outer core which, in the absence of proline, appears to be highly water dependent (Fig. 4). A full elastic recovery was observed under ambient conditions due to the high degree of order, and therefore strength at a local scale stemming from the cooperative rupture of hydrogen bonds described above and in.[32,33] The reversible disorder caused by immersion in water (Fig. 6) leads to a plastic effect, similar to that of the inner core. That is, the mechanical behaviour of the outer core is affected by disorder in the same way as the inner core, but the outer core does not possess the inherent disorder of the inner core under ambient conditions. The changes in behaviour after controlled humidification suggests that the disorder in the inner core acts as a reservoir, providing binding sites for the water, and thus creating a mechanism for the high toughness observed in bulk mechanical investigations.[14] The outer core does not provide this mechanism and, rather than contributing to toughness, is more likely to play a dominant role in the stiffness of the fibre, and is responsible for the linearity of the stress-strain behaviour in the elastic region. We speculate that the inner core region will exhibit a 'J' shaped stress-strain curve under ambient conditions, similar to that observed in bulk studies of supercontracted fibres.[14,34]

Taking up nearly a third of the fibre's volume,[1] the very different behaviour of the outer core is likely to play an important protective role, with its higher hardness and stiffness complementing the tough, impact absorbing inner core similarly to differentially hardened metal in gears, knives and swords, and has been synthetically introduced to increase toughness in biological systems.[35,36] These interpretations of the action of water in spider silk mechanics are limited to small strain behaviour. It is difficult to extrapolate to large-strain behaviour, particularly as the role of water after the conversion to a rubber-like elasticity during yield and later strain hardening[5,37] is likely to change considerably.

The main functional difference between the two proteins, Spidroin I and II, appears to be the ability of Spidroin II to retain water (see also Creager *et al.*[12]). Once the effect of water has been nullified either by saturation (Fig. 4b) or expulsion by applied stress (unloading curves, Fig. 4a and b), they have very similar deformation mechanisms at small strains, with a small contribution from the proline in the Spidroin II. The effect of proline on the mechanical behaviour can be decoupled from that of water by considering the loading curves of the wet samples (Fig. 4b). Here, the water-saturated, proline-rich inner core is only slightly softer than the water-saturated, proline-deficient outer core, with the difference in area between the loading and unloading curves for the two regions showing the dissipation of energy resulting from the presence of proline. The difference in energy dissipated by the proline appears small (21%), relative to that dissipated by the action of water in the inner core under either wet or ambient conditions.

The similar behaviour of the wet inner and outer cores (Fig. 4b) indicates that the action of bound water is critical in load carriage, providing sacrificial amide-water bonds that can be broken to dissipate energy, allowing local strains as the protein chains are pulled into a more ordered configuration and the sacrificial bond is replaced by a stronger and more direct amide-amide bond. Once restructuring has occurred, through disordering by immersion in water or ordering by applied stress, the two proteins are virtually identical from a mechanical perspective. This sacrificial bonding has been observed in the highly disordered capture silk of Araneus spiders[13] and in recombinant dragline silk,[38] using AFM to apply tensile loads to individual proteins. Although these studies provide an interesting insight into silk protein unfolding, the single molecule tests that they employed do not retain the packing conditions existing *in situ* and consequently, are unable to relate their findings to water or the self-repair of hydrogen bonds as the material is restructured under stress. The strength of these sacrificial bonds can, however, be related to the stiffness of the fibre and the softening observed after saturation with water.[8]

The critical role of water in the small strain mechanics of spider silk, the vastly different behaviours of inner and outer core silk under ambient conditions and their similarity under wet conditions, provide some insight into the stress-processing and energy dissipation mechanisms that underlie its remarkable mechanical properties. It may also build on our current understanding of this and other biological fibres such as collagen, elastin and keratin. In this context, our results indicate that the selective binding of water to proteins controls their mechanical behaviour by dictating the level of order and therefore the potential for energy dissipation, restructuring and self-repair.

Building upon this conclusion, we speculate on the impact of the X-ray scattering and indentation results for the development of mechanically robust synthetic silks as biomaterials, which will require compensation for the effects of water.[39] Rather than synthesizing a material to recreate the properties of spider silk, we argue that it is better to synthesize a stiffer, more hydrophobic material that will restructure in wet conditions to provide the water-dominated sacrificial bonding, energy processing and self-repair mechanisms of the inner core material, yet retain the stiff, elastic outer core behaviour that is lost in natural fibres. By looking beyond spider silk mechanics to consider the ordered structures that provide strength and stiffness in wet fibres such as collagen and elastin, it may be possible to recreate, *in vivo*, the delicate balance of properties that make spider silk such a formidable material in ambient conditions.

Outside of the biological environment, the sacrificial toughening mechanisms in the inner core material, and the complementary matching of inner and outer core properties may provide a target for biomimicry. In this respect, a composite can be designed, using a stiff material to carry 'design' loads coupled with a high toughness sacrificial material for one-off extreme loads in seatbelts, bullet proof vests, structural cables in airplanes, construction for earthquake resistance, and other safety applications.

Acknowledgements

This work was supported by grants from the NIHR Biomedical Research Unit into Musculoskeletal Disease, University of Oxford, and The Ministry for Foreign Affairs of Italy (Direzione Generale per la Promozione e la Cooperazione Culturale) and MDEIE (Quebec) under the framework of the Italy-Québec Joint Laboratory in Nanostructured Materials for Energy, Catalysis and Biomedical Applications. C.P.B. acknowledges the Fonds de la Recherche en Santé Québec, Canada for a personal fellowship. J.M. acknowledges the Natural Science and Engineering Research Council (NSERC) of Canada for a postdoctoral fellowship. F.R. is grateful to the Canada Research Chairs program for partial salary support.

References

1 A. Sponner, *et al.*, Composition and Hierarchical Organisation of a Spider Silk, *PLoS One*, 2007, **2**(10), e998.
2 M. Xu and R. V. Lewis, Structure of a protein superfiber: spider dragline silk, *Proc. Natl. Acad. Sci. U. S. A.*, 1990, **87**, 7120–7124.
3 F. Vollrath and D. Porter, Spider Silk as Archetypal Protein Elastomer, *Soft Matter*, 2006, **2**, 377–385.
4 F. Vollrath and D. Porter, Spider silk as a model biomaterial, *Appl. Phys. A: Mater. Sci. Process.*, 2006, **82**, 205–212.
5 D. Porter, F. Vollrath and Z. Shao, Predicting the mechanical properties of spider silk as a model nanostructured polymer, *Eur. Phys. J. E*, 2005, **16**, 199–206.
6 I. Krasnov, *et al.*, Mechanical Properties of Silk: Interplay of Deformation on Macroscopic and Molecular Length Scales, *Phys. Rev. Lett.*, 2008, **100**, 048104.
7 M. E. Rousseau, D. Hernandez Cruz, M. M. West, A. P. Hitchcock and M. Pezolet, Nephila clavipes Spider Dragline Silk Microstructure Studied by Scanning Transmission X-ray Microscopy, *J. Am. Chem. Soc.*, 2007, **129**, 3897–3905.
8 R. W. Work, Viscoelastic Behaviour and Wet Supercontraction of Major Ampullate Silk Fibres of Certain Orb-Web-Building Spiders (Araneae), *J. Exp. Biol.*, 1985, **118**, 379–404.

9 A. Gliovi, T. Vehoff, R. J. Davies and T. Salditt, Strain Dependent Structural Changes of Spider Dragline Silk, *Macromolecules*, 2008, **41**, 390–398.
10 P. Papadopoulos, J. Solter and F. Kremer, Hierarchies in the structural organization of spider silk—a quantitative model, *Colloid Polym. Sci.*, 2009, **287**, 231–236.
11 T. Seydel, *et al.*, Increased molecular mobility in humid silk fibers under tensile stress, *Phys. Rev. E: Stat., Nonlinear, Soft Matter Phys.*, 2011, **83**, 016104.
12 M. S. Creager, *et al.*, Solid-State NMR Comparison of Various Spiders' Dragline Silk Fiber, *Biomacromolecules*, 2010, **11**, 2039–2043.
13 N. Becker, *et al.*, Molecular nanosprings in spider capture-silk threads, *Nat. Mater.*, 2003, **2**, 278–283.
14 M. Denny, The physical properties of spider's silk and their role in the design of orb-webs, *J. Exp. Biol.*, 1976, **65**, 483–506.
15 H. Amenitsch, *et al.*, Performance and First Results of the ELETTRA High-Flux Beamline for Small-Angle X-ray Scattering, *J. Appl. Crystallogr.*, 1997, **30**, 872–876.
16 A. Hammersley, *Fit2D Software*, ESRF, Grenoble, Available at http://www.esrf.eu/computing/scientific/FIT2D/.
17 A. Fischer-Cripps, *Nanoindentation*, Springer-Verlag, New York, 2nd edn, 2004.
18 J. O. Warwicker, Comparative studies of fibroins 2. crystal structures of various fibroins, *J. Mol. Biol.*, 1960, **2**, 350–362.
19 A. Glisovic and T. Salditt, Temperature dependent structure of spider silk by X-ray diffraction, *Appl. Phys. A: Mater. Sci. Process.*, 2007, **87**, 63–69.
20 C. Riekel and F. Vollrath, Spider silk fibre extrusion: combined wide- and small-angle X-ray microdiffraction experiments, *Int. J. Biol. Macromol.*, 2001, **29**, 203–210.
21 C. Branden & J. Tooze, *Introduction to protein structure*, Garland Publishing Inc., New York, 1991.
22 R. Work and N. Morosoff, A physico-chemical study of the supercontraction of spider major ampullate silk fibers, *Text. Res. J.*, 1982, **52**, 349–356.
23 Y. Liu, Z. Shao and F. Vollrath, Relationships between supercontraction and mechanical properties of spider silk, *Nat. Mater.*, 2005, **4**, 901–905.
24 D. Porter and F. Vollrath, The role of kinetics of water and amide bonding in protein stability, *Soft Matter*, 2008, **4**, 328–336.
25 F. Vollrath and D. P. Knight, Liquid crystalline spinning of spider silk, *Nature*, 2001, **410**, 541–548.
26 P. Papadopoulos, J. Solter and F. Kremer, Structure-property relationships in major ampullate spider silk as deduced from polarized FTIR spectroscopy, *Eur. Phys. J. E*, 2007, **24**, 193–199.
27 N. Du, *et al.*, Design of Superior Spider Silk: from Nanostructure to Mechanical Properties, *Biophys. J.*, 2006, **91**, 4528–4535.
28 A. H. Simmons, C. A. Michal and L. W. Jelinski, Molecular orientation and two-component nature of the crystalline fraction of spider dragline silk, *Science*, 1996, **271**, 84–87.
29 J. M. Gosline, P. A. Guerette, C. S. Ortlepp and K. N. Savage, The mechanical design of spider silks: From fibroin sequence to mechanical function, *J. Exp. Biol.*, 1999, **202**, 3295–3303.
30 K. N. Savage and J. M. Gosline, The role of proline in the elastic mechanism of hydrated spider silks, *J. Exp. Biol.*, 2008, **211**, 1948–1957.
31 P. Cordier, F. Tournilhac, C. Soulié-Ziakovic and L. Leibler, Self-healing and thermoreversible rubber from supramolecular assembly, *Nature*, 2008, **451**, 977–980.
32 S. Keten and M. J. Buehler, Geometric Confinement Governs the Rupture Strength of H-bond Assemblies at a Critical Length Scale, *Nano Lett.*, 2008, **8**, 743–748.
33 S. Keten and M. J. Buehler, Strength limit of entropic elasticity in beta-sheet protein domains, *Phys. Rev. E: Stat., Nonlinear, Soft Matter Phys.*, 2008, **78**, 061913.
34 K. N. Savage and J. M. Gosline, The effect of proline on the network structure of major ampullate silks as inferred from their mechanical and optical properties, *J. Exp. Biol.*, 2008, **211**, 1937–1947.
35 S. M. Lee, *et al.*, Greatly Increased Toughness of Infiltrated Spider Silk, *Science*, 2009, **324**, 488–492.
36 M. J. Harrington, A. Masic, N. Holten-Andersen, J. H. Waite and P. Fratzl, Iron-Clad Fibers: A Metal-Based Biological Strategy for Hard Flexible Coatings, *Science*, 2010, **328**, 216–220.
37 D. Porter and F. Vollrath, Silk as a Biomimetic Ideal for Structural Polymers, *Adv. Mater.*, 2009, **21**, 487–492.
38 E. Oroudjev, *et al.*, Segmented nanofibers of spider dragline silk: Atomic force microscopy and single-molecule force spectroscopy, *Proc. Natl. Acad. Sci. U. S. A.*, 2002, **99**, 6460–6465.
39 C. P. Brown, F. Rosei, E. Traversa and S. Licoccia, Spider silk as a load-bearing biomaterial: tailoring mechanical properties *via* structural modifications, *Nanoscale*, 2011, **3**, 870–876.
40 S. Keten and M. J. Buehler, Nanostructure and molecular mechanics of dragline spider silk protein assemblies, *J. Roy. Soc. Interface*, 2010, **7**, 1709–1721.